Geophysical Research Letters

RESEARCH LETTER
10.1029/2024GL113940

Yucatan Hurricane Activity Highlights Common Era Tropical Cyclone Dipole

Richard M. Sullivan[1], Peter J. van Hengstum[2,3], Elizabeth J. Wallace[1], Sloan Coats[4], Jeffrey P. Donnelly[5], Robert Korty[6], Shawna N. Little[7], Martin G. Maas Vargas[8], Luis Mejia-Ortiz[9], Eduard G. Reinhardt[10], Courtney Schumacher[6], Anne E. Tamalavage[11], and Tyler S. Winkler[5]

[1]Department of Earth and Ocean Sciences, Old Dominion University, Norfolk, VA, USA, [2]Department of Oceanography, Texas A&M University, College Station, TX, USA, [3]Department of Marine and Coastal Environmental Science, Texas A&M University at Galveston, Galveston, TX, USA, [4]Department of Earth Sciences, University of Hawaii, Honolulu, HI, USA, [5]Geology & Geophysics, Woods Hole Oceanographic Institution, Woods Hole, MA, USA, [6]Department of Atmospheric Sciences, Texas A&M University, College Station, TX, USA, [7]Department of Marine Biology, Texas A&M University at Galveston, Galveston, TX, USA, [8]Colegio de Bachilleres Plantel Bacalar, Quintana Roo, Mexico, [9]División de Desarrollo Sustentable, Universidad de Quintana Roo, Quintana Roo, Mexico, [10]School of Geography and Earth Sciences, McMaster University, Hamilton, ON, Canada, [11]Smithsonian Environmental Research Center, Edgewater, MD, USA

Key Points:

- Common Era tropical cyclone activity for the Yucatan was reconstructed from blue hole sediments
- Yucatan TC activity is frequently antiphased with storminess for the northeast United States, indicating an apparent Atlantic TC-dipole
- Tropical cyclone activity over the Yucatan varies concurrently with shifts in the Intertropical Convergence Zone

Supporting Information:

Supporting Information may be found in the online version of this article.

Correspondence to:

R. M. Sullivan,
rsulliva@odu.edu

Citation:

Sullivan, R. M., van Hengstum, P. J., Wallace, E. J., Coats, S., Donnelly, J. P., Korty, R., et al. (2025). Yucatan hurricane activity highlights Common Era tropical cyclone dipole. *Geophysical Research Letters*, *52*, e2024GL113940. https://doi.org/10.1029/2024GL113940

Received 3 DEC 2024
Accepted 30 AUG 2025

Author Contributions:

Conceptualization: Peter J. van Hengstum, Robert Korty, Luis Mejia-Ortiz, Courtney Schumacher
Formal analysis: Richard M. Sullivan
Funding acquisition: Peter J. van Hengstum, Jeffrey P. Donnelly, Robert Korty, Luis Mejia-Ortiz, Courtney Schumacher
Investigation: Richard M. Sullivan, Peter J. van Hengstum, Elizabeth J. Wallace, Sloan Coats, Jeffrey P. Donnelly, Shawna N. Little, Martin G. Maas Vargas, Luis Mejia-Ortiz, Eduard G. Reinhardt, Anne E. Tamalavage, Tyler S. Winkler
Supervision: Peter J. van Hengstum
Visualization: Richard M. Sullivan, Peter J. van Hengstum
Writing – original draft: Richard M. Sullivan

Abstract Tropical cyclone (TC) impacts along the western Atlantic and Caribbean margin are not spatially uniform. Proxy based reconstructions of Common Era TC activity highlight this non-uniform distribution at centennial-millennial timescales. However, the sparse geographic scope of these reconstructions impedes our assessment of TC landfalls across broader spatial domains. This work presents a compilation of new and existing TC reconstructions from the Yucatan Peninsula for comparison with a contemporaneous compilation from New England, showing that these regions occupy distal nodes of a low-frequency TC dipole. Increased Yucatan (New England) storminess is closely linked to intervals of Northern Hemisphere warming (cooling) and the expansion (contraction) of the Intertropical Convergence Zone, suggesting that secular shifts in the mean climate state mediate dipole orientation.

Plain Language Summary Coastal ponds, lagoons, blue holes, and sinkholes can preserve evidence of nearby tropical cyclone (TC) activity through storm-driven sediment deposits. By identifying variations in these deposits, we can reconstruct past TC activity, extending our understanding of storm behavior back centuries. In this study, we present a new TC reconstruction from the Yucatan. When considered with previously published TC records throughout the northwest Atlantic, our findings reveal that Yucatan TC activity was often the opposite of activity in the northeast US at centennial timescales. This study demonstrates the broad spatial extent of this pattern in TC landfalls and shows that larger climate shifts over the last two millennia likely influenced multi-decadal changes in TC activity.

1. Introduction

Tropical cyclones (TCs) recurrently threaten coastal communities along the northwest Atlantic, Gulf of Mexico, and the small island states of the Caribbean basin, though TCs pose unequal risks throughout these regions (Kossin et al., 2010). Furthermore, prior work examining the impact of recent anthropogenic-induced climate change on Atlantic TCs has primarily focused on the US coastline, noting that the susceptibility of the region to storm strikes generally increases concomitantly with regional warming (Dailey et al., 2009; Garner et al., 2021; Weaver & Garner, 2023). Additionally, the mid-Atlantic portion of the US coast often sees an increase in storminess concurrent with a decrease in the number of Gulf or Caribbean storms due to changes in genesis location and steering flow (Colbert et al., 2013). However, few studies consider how broader regional susceptibility to landfalling TCs may have varied prior to modern warming. This is critical for deciphering the impact that naturally and anthropogenically forced variability has on long-term TC hazards. This gap in knowledge underscores the limitations of the modern observational record, which, by nature of its brevity, precludes resolving multi-decadal to multi-centennial TC activity and related drivers (Landsea et al., 2006). This limits our capacity to fully evaluate potential TC risks under different climate states. Therefore, addressing these deficiencies requires longer duration records of storm activity that more accurately reflect naturally forced TC climatology.

Writing – review & editing: Richard M. Sullivan, Peter J. van Hengstum, Elizabeth J. Wallace, Sloan Coats, Jeffrey P. Donnelly, Robert Korty, Shawna N. Little, Luis Mejia-Ortiz, Eduard G. Reinhardt, Courtney Schumacher, Anne E. Tamalavage, Tyler S. Winkler

Sediment-based paleo-proxy reconstructions of past TC activity offer an alternate method of investigating storm frequency and landfalling distribution prior to modern observations. Wind and waves associated with strong TCs can remobilize existing sedimentary reserves for subsequent archival within adjacent lacustrine, marsh, or lagoonal settings where these deposits become stratigraphically preserved within the fine-grain background sedimentary matrix (Ercolani et al., 2015; Liu & Fearn, 1993; Winkler et al., 2023). However, the fidelity of a sediment-based reconstruction depends on factors such as proxy sensitivity (Otvos, 2011) and the unique characteristics of the individual sites (Goslin & Clemmensen, 2017; Lin et al., 2014), which, along with chronostratigraphic uncertainties, may contribute to disagreement between TC reconstructions. Furthermore, recent work has proposed that atmospheric stochasticity may limit the capacity of a single TC reconstruction to reflect large scale climate variability and secular trends (Wallace et al., 2020). Though these explanations may account for specific and localized aspects of TC record disagreement, recurrent patterns observed among proximal (Ercolani et al., 2015) and distal (Donnelly et al., 2015; Elsner et al., 2000; van Hengstum et al., 2016) reconstructions suggest a degree of low-frequency regional coherency among landfalling TCs. This potential synchronicity may be further clarified by combining proximal TC reconstructions into regional compilations to average out site-specific variability (Wallace, Donnelly, et al., 2021; Winkler et al., 2023). While this approach has been previously applied to localities where multiple sub-decadally resolved records have been developed (e.g., The Bahamas, northeast US, and eastern Gulf of Mexico), a lack of highly resolved TC reconstructions from the western Caribbean has impeded our ability to properly assess the spatiotemporal characteristic of naturally forced Atlantic TCs over longer timescales.

Here we present a new compilation of Common Era TC activity derived from sediment cores recovered from the eastern Yucatan peninsula, a region where comparatively few high-fidelity multi-millennial TC reconstructions have been published to date (Wallace, Dee, & Emanuel, 2021). Comparing our new compilation with existing TC paleo-proxy compilations from the northeast US and The Bahamas reveals opposing intervals of multi-decadal storminess that are most apparent during substantial Northern Hemisphere temperature perturbations, such as during the Medieval Warm Period (MWP; ~800 to 1400 CE) and Little Ice Age (LIA: ~1450 to 1850 CE). This alternating TC response is concurrent with meridional shifts in the northern edge of the Intertropical Convergence Zone (ITCZ), suggesting that persistent and large hemispheric temperature gradients exert a non-uniform influence on the landfalling distribution of Atlantic TCs at multi-decadal to centennial scales. Ultimately, this work reveals that naturally forced changes to the mean climate state drive regionally coherent, but divergent, responses to the landfall distribution of TCs along the west Atlantic margin.

2. Yucatan Peninsula

The Yucatan Peninsula is ideally positioned to examine west Atlantic TC activity since it is highly susceptible to TC impacts (Sullivan et al., 2022; Winkler et al., 2020) (Figure 1). The peninsula has been impacted by 20 major TC events (≥Cat 3) since 1900 CE, with >80% making landfall between August and October. Yucatan hydroclimate is influenced by multiple interacting modes of climate variability, including the ITCZ (Aragón-Moreno et al., 2018; Pollock et al., 2016; Ridley et al., 2015), the Caribbean Low-Level Jet (Gamble et al., 2008; Martin & Schumacher, 2011; Martinez et al., 2019), the El Niño/Southern Oscillation (ENSO) (Giannini et al., 2001), temperature gradients between the Atlantic and Pacific basins (Bhattacharya & Coats, 2020), and meridional displacements and western expansion of the North Atlantic Subtropical High (NASH) (Díaz-Esteban & Raga, 2018; Sullivan et al., 2021). While numerous rainfall reconstructions exist for the region (Curtis et al., 1996; Kennett et al., 2012; Medina-Elizalde et al., 2010) the mechanisms mediating local water balance variability likely differ from those influencing TC characteristics, including track and genesis (Cook et al., 2012; Emanuel, 1999; Kossin et al., 2010; Oglesby et al., 2010). Therefore, proper assessment of past Yucatan hydroclimate volatility requires that TC activity and rainfall be considered separately.

3. Study Site

Coarse sedimentary particles archived within the blue holes, sinkholes, or cenotes can provide evidence of proximal TC passage throughout the tropical North Atlantic (Denommee et al., 2014; Sullivan et al., 2022; van Hengstum et al., 2016) and Pacific oceans (Bramante et al., 2020). TCs increase local hydrodynamics and wave climate, which re-mobilizes coarse materials that then become redeposited within nearby karst basins as flow rates attenuate. These storm-induced deposits remain texturally distinct from the fine-grained authigenic

10.1029/2024GL113940

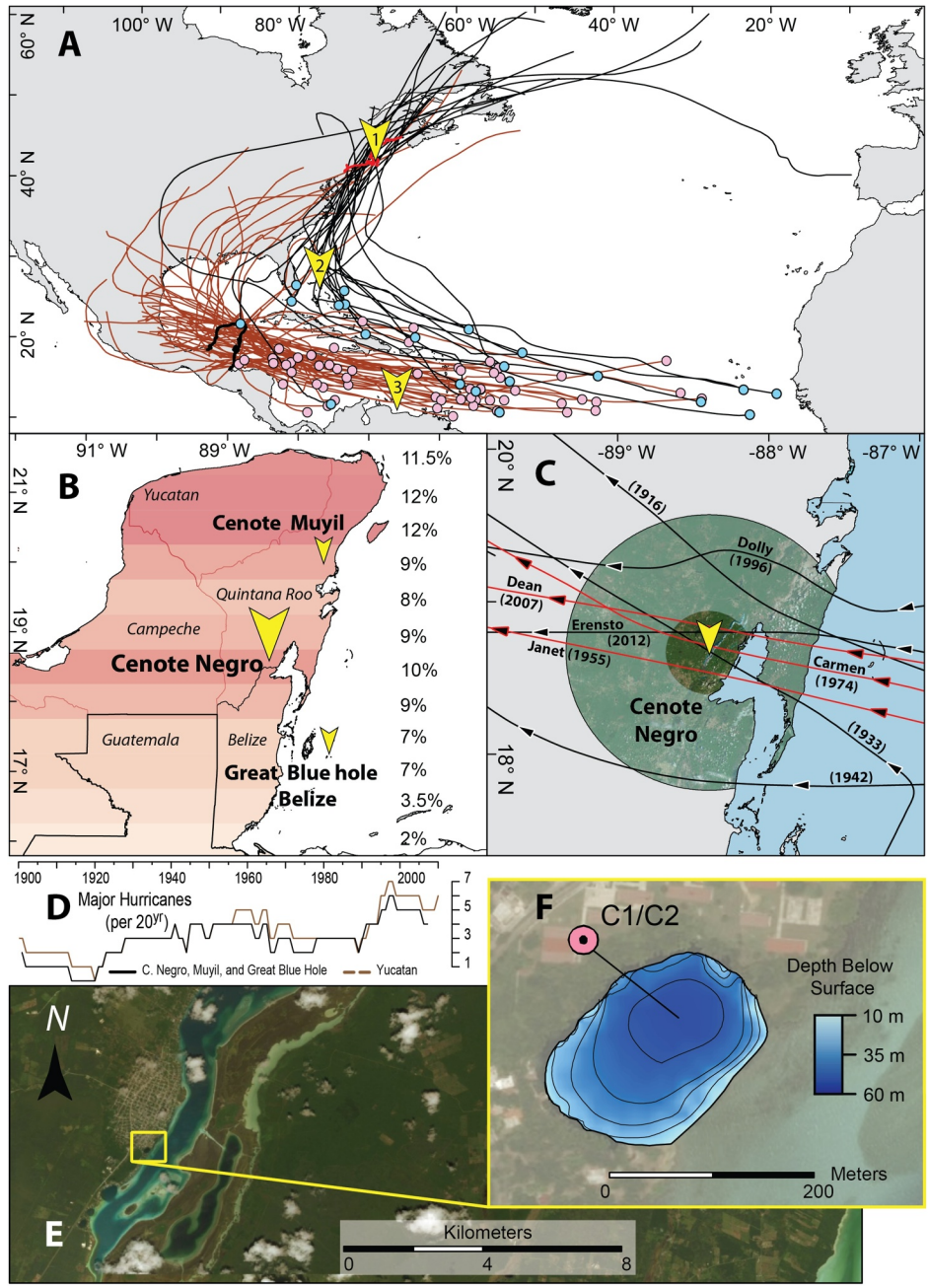

Figure 1. (a) All recorded TCs (≥Cat 1) that have made landfall on the Yucatan (brown) and New England (black) since 1900 CE. Pink (blue) circles indicate genesis locations for Yucatan (New England) storms. The Yucatan is outlined in black and New England coast is shown in red. Yellow chevrons indicate locations of other paleo records discussed in this work; (1) Salt Pond/NE TC reconstructions (Donnelly et al., 2015; Winkler et al., 2023), (2) The Bahamas (Winkler et al., 2023), and (3) Cariaco Basin %Ti flux (Haug et al., 2001) in South America. (b) Yucatan hurricane reconstructions discussed in this study (chevrons). Colored bars depict percent of tropical storms or greater (binned at 0.5° latitude) from NOAA's Best Track Data set (Knapp et al., 2010) intersecting with Yucatan Peninsula over a 100-year period between 1920 and 2020 CE. Country borders are outlined in black and Mexico state borders in red. (c) Hurricanes that have impacted Laguna Bacalar since 1900 CE. Major Hurricanes (≥ Cat 3) passing within 100 km shown in red, Cat 1 and 2 events in black. Note all recent major events have passed within 30 km of the cenote. (d) 20-year return interval for major hurricanes impacting the Yucatan since 1900 CE (black line) and combined counts of observed storms at Cenote Negro, Muyil, and Lighthouse Reef Blue Hole (gold line). Note that the major Yucatan storm impacts correlate with the storms impacting the three locations ($r = 0.93$, $p < 0.001$), indicating that this combination faithfully reflects multidecadal storm variability over the region. (e) Aerial view of Laguna Bacalar and Cenote Negro (in yellow). (f) Bathymetric map of Cenote Negro. Core locations are also shown.

carbonate or sapropel that otherwise comprise the typical background sediment matrix of karst basins on carbonate landscapes.

Laguna Bacalar is a sulfate-rich (Pérez et al., 2011), oligotrophic, ground water fed, freshwater lake located in southern Quintana Roo, Mexico (Gischler et al., 2008; Johnson et al., 2018) (Figure 1). The lake extends NNE for ∼40 km, has an average width of ∼2 km, and a maximum depth of 15 m. A prominent lineament of 4 cenotes (cenotes Azul, Cocalitos, Esmerelda, and Negro) is found on the lake's western margin, with cenote Xel-Ha connected to the south. Laguna Bacalar is saturated with respect to calcite ($CaCO_3$) (Perry et al., 2002) with benthic sediment dominated by a fine grained lacustrine marl matrix interspersed with carbonate shells. In general, lacustrine marl sedimentation may occur when carbonate-saturated groundwater decalcifies from evaporation, by biocarbonate assimilation from algae or macrophytes, or when CO_2 degases from the mixing of thermally distinct water bodies (Holmes et al., 1995; Street-Perrott et al., 1993). It is likely that similar processes are driving lacustrine marl precipitation within Laguna Bacalar. The lake contains a steady northward current originating from the Xel-Ha cenote (Johnson et al., 2018) that drives thermal mixing by exporting groundwater into the lake and transporting fine grain sediment northward for deposition into the adjacent quiescent cenotes.

The northernmost cenote, Cenote Negro (18.667°N, 88.394°W), is 51 m deep (dysoxic below ∼10 m, Text S1 in Supporting Information S1), 140 m by 190 m wide and connected to the lagoon by a shallow (∼2 m) but wide (120 m) sill on the eastern edge. Bathymetric mapping (Figure S1 in Supporting Information S1) indicates steep sides that may contain overhangs and connections to larger cave networks, though direct observations were not available. The western perimeter abuts a steep hill with a maximum elevation of ∼18 m that slopes down to the water's edge encircling ∼60%–70% of the cenote from the NNE to ∼SW. This topography offers some protection from storms passing to the north but leaves the cenote vulnerable to storms passing to the south. Specifically, the NNE orientation of the lagoon means that the greatest available fetch is along that axis, thus the maximum wave heights are generated by storms passing to the south.

Since 1900 CE eight hurricanes (≥Cat 1) have passed within 100 km of Cenote Negro with all three recorded major hurricanes (≥Cat 3) passing within 30 km of the cenote (Figure 1). Of these eight events, Hurricane Carmen (1974 CE) and an unnamed Cat 1/TS event in 1933 CE passed directly over the cenote. Hurricanes Dean (2007 CE) and Ernesto (2012 CE) both passed to the north but remained within 20 km at the nearest approach. Hurricane Janet (1955 CE) passed ∼18 km south of the cenote with maximum recorded winds of 150 kts, a speed potentially capable of generating waves exceeding 8 m along the longest stretch of uninterrupted fetch within the lagoon (∼11 km) (Carter, 1982).

4. Cenote Negro TC Record

Two continuous sediment cores (>7 m long) were recovered from Cenote Negro in 2017 (Figure 1, Figure S1 in Supporting Information S1) using a submersible vibracoring system (see Text S2 in Supporting Information S1 for further details). The sedimentary infill of the cenote is dominated by fine-grained authigenic lacustrine marl interspersed with coarse-grained (>63 μm) carbonate sand, gastropod and bivalve shell material (e.g., *Hydrobia, Pyrgophorus*), and terrestrial organic detritus (Figures S2 and S3; Texts S3 and S4 in Supporting Information S1). The dysoxic conditions at the base of the cenote (Figure S1 in Supporting Information S1) and well-preserved horizontal bedding suggest limited bioturbation and that gastropod and bivalve shell material was likely allochthonous rather than preserved in situ.

Age/depth models (Methods S5 in Supporting Information S1) revealed that core 1 (C1) encompassed 2,358 years (basal age 341 BCE), and core 2 (C2) spanned 2,485 years (basal age 468 BCE) (Figure S4 in Supporting Information S1). Sedimentation rates remained constant at the core site (C1: 3.8 years/cm; C2: 3.7 years/cm) with no identifiable hiatuses or significant slump features. C1 and C2 each contain coarse sediment beds that satisfy the criteria for anomalous deposition (as defined in Text S6 of Supporting Information S1). These beds are interpreted as evidence of localized, ephemeral increases in hydrodynamics during near-to-direct TC passage, which can remobilize nearby sediments due to heightened wind and wave energy (Figure S5, Text S7 in Supporting Information S1). C1 (C2) contains a total of 51 (43) TC deposits. This equates to an average rate of 2.2 events per century (46.2 years event^{-1}) as recorded by C1, and a rate of 1.7 events per century (57.8 years event^{-1}) in C2. These differences in the number of storm deposits contained within the two cores are likely due to basin specific geometries that may prevent uniform distribution of sediment following a high-energy depositional event. Alternatively, consecutive events occurring below the temporal resolution of the sediment record may yet remain

individually discernible in one core despite appearing as a single event in the other, producing minor discrepancies in the total number of recorded storms.

Since the frequency of these events varies within both records, we can highlight centennial variability in storm occurrence by summing events within a 100-year moving window. Intervals where storm occurrence deviates from the mean by $>1\sigma$ are considered intervals of anomalously high or low TC activity. This method yields an average frequency ($\pm1\sigma$) of 2.2 ± 1.7 events/century for C1 and 1.7 ± 1.3 events/century for C2 and gives us 1σ thresholds in C1 of 3.8 to 0.4 TCs per century and 3.0 to 0.4 TCs per century in C2. Frequency counts outside this range are considered anomalously active or inactive periods. Though the difference in the number of storm deposits between the cores is low, it can be minimized further by consolidating the individual frequency counts into a single record to provide a more accurate representation of the cenote's TC history (Figure S6 in Supporting Information S1). For the purposes of discussion, successive active/inactive intervals (intervals where TC frequency deviates from the mean by $>1\sigma$) exceeding 10 years in duration and occurring within 50 years of each other can be grouped into clusters. The combined C1 and C2 frequency record, presented as the mean *Z*-score (Figure 2, Figure S6 in Supporting Information S1), contains five active clusters (420 BCE to 330 BCE, 200 BCE to 170 BCE, 110 CE to 400 CE, 1440 CE to 1480 CE, and 1910 CE to Present) and five inactive clusters (570 CE to 860 CE, 970 CE to 1020 CE, 1220 CE to 1300 CE, 1530 CE to 1600 CE, and 1760 CE to 1830 CE).

5. Yucatan Regional Compilation

Considering that paleotempestological reconstructions from a single location may be affected by site-specific factors, and that the frequency of landfalling TCs varies meridionally across the peninsula (Figure 1), we must incorporate sites across a latitudinal range over the Yucatan to characterize regional TC activity. A ~2,200 years-long reconstruction from Cenote Muyil (Sullivan et al., 2022), ~170 km north of Laguna Bacalar (Figure 1), is an ideal companion for compilation since both records encompass the entirety of the Common Era, have sub-decadal resolutions, and are sensitive to similar categories of storms (see Text S8 in Supporting Information S1). Similarly, a previously published record from Lighthouse Reef, Belize (Denommee et al., 2014) provides additional evidence of regional storminess at sub-decadal scales since the Medieval Warm Period (MWP; ~800 to 1400 CE). Modern observations of major hurricanes (≥category 3 on the Saffir-Simpson scale) impacting the Yucatan positively covary with the frequency of observed events striking these three cenotes ($r = 0.93$, $p < 0.001$) at multidecadal (20 years) timescales (Figure 1), which provides confidence that the new regional compilation characterizes prehistoric Yucatan TC variability.

We developed the Yucatan Regional Compilation (Figure 2, Text S8 in Supporting Information S1) by summing the standardized centennial TC records from the three contributing sites. An alternate method, which sums the age probability distribution functions of individual events in each record, was also applied to preserve the age uncertainties inherent to each chronology (Figure S7 in Supporting Information S1). Our approach, coupling multiple sites from within a region and focusing on TCs at centennial-scales, accounts for intrinsic weather-related TC variability (Kortum et al., 2023) and permits coherent patterns to emerge from the higher-frequency noise. These compilations indicate three persistent (>50 years) intervals of anomalously low TC activity (I1: ~550 CE to 750 CE, I2: 1460 to 1660 CE, and I3: 1700 to 1860 CE) and six persistent intervals of anomalously high TC activity (A1: ~250 BCE to 140 BCE, A2: 100 BCE to 60 CE, A3: 250 to 310 CE, A4: 890 to 1010, A5: 1250 to 1410 CE, and A6: ~1920 to present). It is unsurprising that the timing of these active and inactive intervals broadly aligns with intervals of persistent northern hemispheric warming, such as during the Roman Warm Period (RWP: ~250 BCE to 400 CE) and modern anthropogenic warming, and cooling during the Late Antiquity Little Ice Age (LALIA: ~530 to 660 CE) and LIA (~1450–1850 CE) respectively. However, an interval contemporaneous with the MWP (~1000 CE to ~1250 CE) experienced centennial TC variability that rarely exceeded the mean. Additionally, the timing of these intervals remains consistent with a previous assessment that the Maya Terminal Classic Phase (a period of widespread sociopolitical destabilization throughout the Maya lowlands ~900 CE) was synchronous with an anomalous increase in TC activity (Sullivan et al., 2022), which may have exacerbated contemporaneous cultural and environmental stressors.

Overall, this new compilation shows (a) a decreasing trend in TC activity from the earliest part of the record moving from the RWP into the LALIA, (b) a marked increase in TCs during the early and late MWP, (c) a sudden decrease in TCs during the LIA with a minor increase in activity in the late 17th/early 18th century, followed by

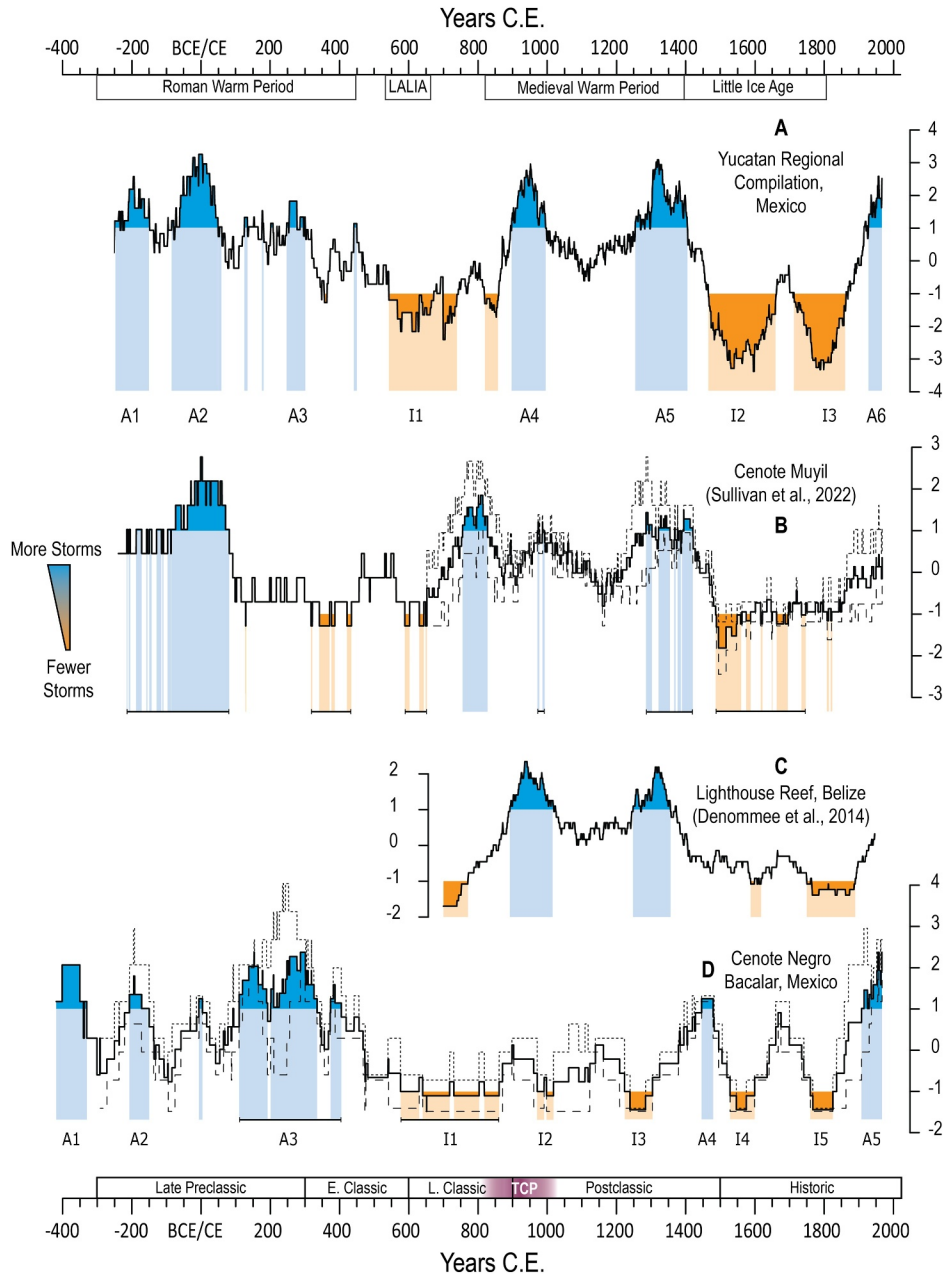

Figure 2. The Yucatan Regional Compilations (a) developed from Cenote Muyil (b), Lighthouse Reef Blue hole (c), and Cenote Negro (d). Blue (orange) shaded regions are intervals where event frequency exceeds (falls below) 1σ, referred to in the main text as Active (A) and Inactive (I) intervals. Dashed lines surrounding the Cenote Negro and Muyil plots indicate maximum and minimum event frequencies for each location. *Y* axes denote *Z*-Score values. Maya cultural phases, including the Terminal Classic Phase (TCP) are listed along the lower year axis.

(a) a strong increasing trend moving into the modern era. This indicates that low-frequency shifts in Yucatan TC activity vary in conjunction with Northern Hemisphere temperature changes.

6. Tropical Cyclone Dipole

Comparison of the Yucatan Regional Compilation with TC reconstructions from New England (Winkler et al., 2023) shows that storminess in these two regions was often antiphased during the Common Era prior to the ~19th century and the onset of modern warming (Figure 3). Increased activity in the Yucatan coincides with

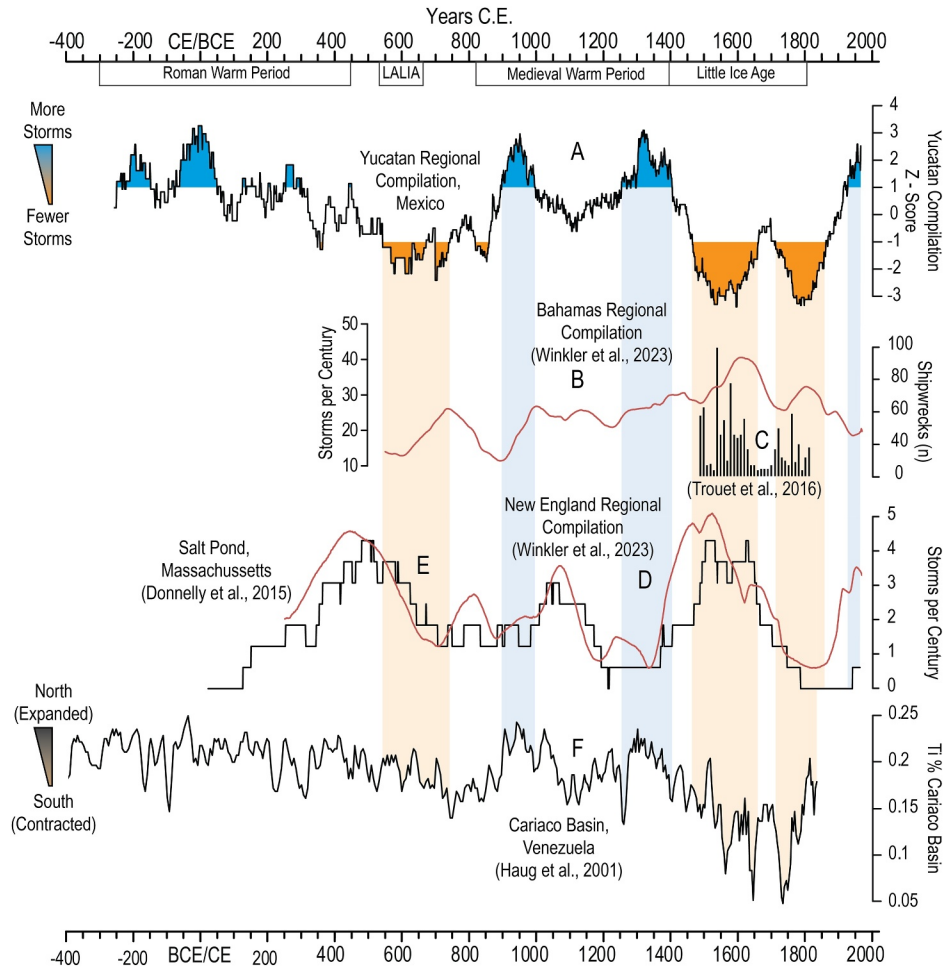

Figure 3. (a) Yucatan Regional Compilation where blue (orange) shaded regions are intervals where Yucatan event frequency exceeds (falls below) 1σ. (b) Bahamas TC compilation (Winkler et al., 2023). (c) Caribbean Shipwreck record (Trouet et al., 2016). (d, e) New England TC compilation in red (Winkler et al., 2023) and the reconstruction from Salt Pond MA in black (Donnelly et al., 2015). (f) Rainfall reconstruction (%Ti) from Cariaco Basin indicative of meridional displacements of the ITCZ (Haug et al., 2001) or ITCZ expansion/contraction (Atwood et al., 2021).

decreased activity in the northeast during the RWP and early and late MWP. Similarly, peak New England TC activity occurs in the 16th century, during the least active period in the Yucatan, and the lull in Yucatan storminess from ~1000 to 1250 CE is contemporaneous with a relative increase in New England TCs. Comparisons between the Yucatan composite and a compilation of Bahamian TC reconstructions show a more distinct antiphased pattern during the LIA, though synchronicity between these regions is less clear during the MWP, indicating that The Bahamas may represent a blend of dipole alignments over time. A similar antiphased pattern is observed between the Yucatan Regional Compilation and a record of Caribbean TC activity during the LIA that was reconstructed from ship logs and historical accounts (Trouet et al., 2016) (Figure 3). Considering that ship records from the colonial era and early 19th century were likely biased toward densely populated regions (e.g., Cuba, Puerto Rico) where ship traffic was more common (Herrera et al., 2004), this record likely characterizes TC activity only within the northern and eastern Caribbean basin. Moreover, since this record shows peak TC activity during the early LIA (similar to New England), we infer that TC frequency in the northern and eastern Caribbean may be more closely linked to storminess along the eastern US than the Yucatan at this interval.

Comparing these records with a sediment-based reconstruction of past ITCZ dynamics from the Cariaco Basin (Haug et al., 2001), derived from changes in terrigenous runoff interpreted as shifts in ITCZ location, shows that increased Yucatan TC activity is largely contemporaneous with a northerly shifted (or potentially wider) ITCZ. Conversely, increases in New England TCs (such as during the early LIA and mid-MWP) are coincident with

southern displacements (or contractions) of the ITCZ. Previous work has shown that hurricane landfalls are partially dependent on cyclogenesis locations (Colbert & Soden, 2012; Kortum et al., 2023), with eastward shifts in genesis corresponding to increases in landfalls along the eastern US coasts. A more northerly or wider ITCZ may encourage cyclogenesis in the western Caribbean or western tropical Atlantic by reducing windshear and increasing low-level vorticity, raising the likelihood that storms impact the Yucatan. Additionally, the NASH, a semi-permanent high-pressure anticyclone known to impact Atlantic hydroclimate during the boreal summer via the geographic extent of its western edge (Li et al., 2012; Martinez et al., 2019) may influence storm track and development in the tropical Atlantic (Liu & Fearn, 2000; Pérez-Alarcón et al., 2021). An expanded NASH would likely impede cyclogenesis within the tropical and subtropical Atlantic due to increased windshear from NASH intensification, while potentially amplifying western steering flow for storms forming in the western part of the Atlantic main development region (Elsner et al., 2000; Malaizé et al., 2011; Pérez-Alarcón et al., 2021). The NASH and ITCZ have been linked to an inverse pattern of hydroclimate variability over the Caribbean (Sullivan et al., 2021), but the role these features have on low-frequency regional TC susceptibility throughout the basin remains unknown.

The mechanisms motivating the increase in TC impacts along the northeast US and Bahamas during the early LIA, concurrent with a southern displacement (or contraction) of the ITCZ, are similarly unclear. Donnelly et al. (2015) hypothesized that this northward shift in TC activity may be related to positive sea surface temperature anomalies in the subtropical northwest Atlantic, which may encourage cyclogenesis off the southeast US. Relatedly, a weaker and more retracted NASH would be less likely to impart westward steering flow to developed storms and may increase the likelihood of Atlantic TCs impacting coasts at higher latitudes. While previous authors have also attempted to link ITCZ displacements (Donnelly et al., 2015; McCloskey & Knowles, 2009; van Hengstum et al., 2016) or NASH geographic variability (Bregy et al., 2022; Scott et al., 2003) to Atlantic TC landfall positions, additional work remains to more thoroughly assess how ITCZ and NASH dynamics have influenced Common Era TC activity.

7. Implications

Projections of future TC variability suggest that landfalls will shift northward due to anthropogenic warming (Kossin et al., 2014; Studholme et al., 2022). In these scenarios, the risk TCs pose to the eastern US will increase while the susceptibility of the Caribbean and Gulf of Mexico to TC impacts may decrease. However, the reconstructions presented here show the opposite relationship over much of the Common Era, with higher (lower) latitude sites experiencing more (fewer) TC landfalls during intervals of reduced global temperatures (e.g., the LIA). This apparent contradiction may derive from differences in the mechanisms driving modern anthropogenic warming relative to past intervals of naturally forced climate variability. Future analyses will more thoroughly assess the drivers of past regional synchronicity.

8. Conclusion

Our study analyzing reconstructed TC variability from multiple locations across the eastern Yucatan Peninsula, reveals a strong linkage between regional storminess and the state of the ITCZ at multi-centennial scales, with a northern/expanded ITCZ concurrent with increased Yucatan TC impacts. Notably, we find evidence of a low-frequency TC dipole between distal nodes in the western Atlantic, characterized by antiphased storm activity between the Yucatan Peninsula and New England at discrete intervals during the Common Era. This work underscores the dynamic interaction between TC behavior and synoptic patterns that vary on climate scales. However, there remains a need for further research to explore the spatial coherency of landfall patterns across the Caribbean region and the Atlantic margin in greater detail, particularly in clarifying the roles of genesis location and steering flow and the influence of other climate modes (e.g., ENSO and the North Atlantic Oscillation) and inter-basin teleconnections over longer, that is, millennial, timescales. Studies such as this provide critical insight and a deeper understanding into the long-term behavior of naturally forced TCs and the climatic mechanisms that influence observed variability.

Conflict of Interest

The authors declare no conflicts of interest relevant to this study.

Data Availability Statement

Data sets generated during this research (grain size, chronology) are available from the National Oceanic and Atmospheric Administration's National Centers for Environmental Information (NCEI) paleoclimatology repository (Sullivan et al., 2024). Support for the Twentieth Century Reanalysis Project version 3 data set is provided by the U.S. Department of Energy, Office of Science Biological and Environmental Research (BER), by the National Oceanic and Atmospheric Administration Climate Program Office, and by the NOAA Earth System Research Laboratory Physical Sciences Laboratory.

Acknowledgments
We dedicate this work to the memory of Dr. Luis Mejia-Ortiz whose contributions furthered our understanding of the Yucatan's unique environmental history and the rich biodiversity of its modern age. Laboratory assistance was provided by Sean Buckelew, Lauren Mennen, and Oscar Cavasos. Fieldwork was supported by Atilano Sandoval. This research was supported by Grants from The Explorer's Club, the Texas A&M University Texas A&M Triads for Transformation Program, the Geological Society of America Graduate Student Research Grant program (EAR-1712071), and Grants to PvH (OCE-1356509, EAR-1833117, EAR-1703087) and JPD (OCE-1903616, EAR-1702946) from the National Science Foundation and to PvH and LM-O from the TAMU-CONAyCT Program. NOAA Global Surface Temperature (NOAAGlobalTemp) data and NOAA/CIRES/DOE 20th Century Reanalysis (V3) provided by the NOAA PSL, Boulder, Colorado, USA, from their website at https://psl.noaa.gov.

References

Aragón-Moreno, A. A., Islebe, G. A., Torrescano-Valle, N., & Arellano-Verdejo, J. (2018). Middle and late Holocene mangrove dynamics of the Yucatan Peninsula, Mexico. *Journal of South American Earth Sciences*, *85*, 307–311. https://doi.org/10.1016/j.jsames.2018.05.015

Atwood, A. R., Battisti, D. S., Wu, E., Frierson, D. M. W., & Sachs, J. P. (2021). Data-model comparisons of tropical hydroclimate changes over the common era. *Paleoceanography and Paleoclimatology*, *36*(7), e2020PA003934. https://doi.org/10.1029/2020PA003934

Bhattacharya, T., & Coats, S. (2020). Atlantic-Pacific gradients drive last millennium hydroclimate variability in Mesoamerica. *Geophysical Research Letters*, *47*(13), e2020GL088061. https://doi.org/10.1029/2020gl088061

Bramante, J. F., Ford, M. R., Kench, P. S., Ashton, A. D., Toomey, M. R., Sullivan, R. M., et al. (2020). Increased typhoon activity in the Pacific deep tropics driven by little ice age circulation changes. *Nature Geoscience*, *13*(12), 806–811. https://doi.org/10.1038/s41561-020-00656-2

Bregy, J. C., Maxwell, J. T., Robeson, S. M., Harley, G. L., Elliott, E. A., & Heeter, K. J. (2022). US Gulf Coast tropical cyclone precipitation influenced by volcanism and the North Atlantic subtropical high. *Communications Earth and Environment*, *3*(1), 164. https://doi.org/10.1038/s43247-022-00494-7

Carter, D. J. T. (1982). Prediction of wave height and period for a constant wind velocity using the JONSWAP results. *Ocean Engineering*, *9*(1), 17–33. https://doi.org/10.1016/0029-8018(82)90042-7

Colbert, A. J., & Soden, B. J. (2012). Climatological variations in North Atlantic tropical cyclone tracks. *Journal of Climate*, *25*(2), 657–673. https://doi.org/10.1175/jcli-d-11-00034.1

Colbert, A. J., Soden, B. J., Vecchi, G. A., & Kirtman, B. P. (2013). The impact of anthropogenic climate change on North Atlantic tropical cyclone tracks. *Journal of Climate*, *26*(12), 4088–4095. https://doi.org/10.1175/jcli-d-12-00342.1

Cook, B. I., Anchukaitis, K. J., Kaplan, J. O., Puma, M. J., Kelley, M., & Gueyffier, D. (2012). Pre-Columbian deforestation as an amplifier of drought in Mesoamerica. *Geophysical Research Letters*, *39*(16). https://doi.org/10.1029/2012gl052565

Curtis, J. H., Hodell, D. A., & Brenner, M. (1996). Climate variability on the Yucatan Peninsula (Mexico) during the past 3500 years, and implications for Maya cultural evolution. *Quaternary Research*, *I*(1), 37–47. https://doi.org/10.1006/qres.1996.0042

Dailey, P. S., Zuba, G., Ljung, G., Dima, I. M., & Guin, J. (2009). On the relationship between North Atlantic sea surface temperatures and US hurricane landfall risk. *Journal of Applied Meteorology and Climatology*, *48*(1), 111–129. https://doi.org/10.1175/2008jamc1871x.1

Denommee, K., Bentley, S., & Droxler, A. (2014). Climatic controls on hurricane patterns: A 1200-y near-annual record from lighthouse reef, Belize. *Scientific Reports*, *4*(1), 3876. https://doi.org/10.1038/srep03876

Díaz-Esteban, Y., & Raga, G. B. (2018). Weather regimes associated with summer rainfall variability over southern Mexico. *International Journal of Climatology*, *38*(1), 169–186. https://doi.org/10.1002/joc.5168

Donnelly, J. P., Hawkes, A. D., Lane, P., MacDonald, D., Shuman, B. N., Toomey, M. R., et al. (2015). Climate forcing of unprecedented intense-hurricane activity in the last 2000 years. *Earth's Future*, *3*(2), 49–65. https://doi.org/10.1002/2014ef000274

Elsner, J. B., Liu, K.-B., & Kocher, B. (2000). Spatial variations in major US hurricane activity: Statistics and a physical mechanism. *Journal of Climate*, *13*, 2293–2305. https://doi.org/10.1175/1520-0442(2000)013<2293:svimus>2.0.co;2

Emanuel, K. A. (1999). Thermodynamic control of hurricane intensity. *Nature*, *401*(6754), 665–669. https://doi.org/10.1038/44326

Ercolani, C., Muller, J., Collins, J., Savarese, M., & Squiccimara, L. (2015). Intense southwest Florida hurricane landfalls over the past 1000 years. *Quaternary Science Reviews*, *126*, 17–25. https://doi.org/10.1016/j.quascirev.2015.08.008

Gamble, D. W., Parnell, D. B., & Curtis, S. (2008). Spatial variability of the Caribbean mid-summer drought and relation to North Atlantic high circulation. *International Journal of Climatology: A Journal of the Royal Meteorological Society*, *28*(3), 343–350. https://doi.org/10.1002/joc.1600

Garner, A. J., Kopp, R. E., & Horton, B. P. (2021). Evolving tropical cyclone tracks in the North Atlantic in a warming climate. *Earth's Future*, *9*(12), e2021EF002326. https://doi.org/10.1029/2021ef002326

Giannini, A., Kushnir, Y., & Cane, M. (2001). Seasonality in the impact of ENSO and the North Atlantic high on Caribbean rainfall. *Physics and Chemistry of the Earth—Part B: Hydrology, Oceans and Atmosphere*, *26*(2), 143–147. https://doi.org/10.1016/s1464-1909(00)00231-8

Gischler, E., Gibson, M. A., & Oschmann, W. (2008). Giant Holocene freshwater microbialites, Laguna Bacalar, Quintana Roo, Mexico. *Sedimentology*, *55*(5), 1293–1309. https://doi.org/10.1111/j.1365-3091.2007.00946.x

Goslin, J., & Clemmensen, L. B. (2017). Proxy records of Holocene storm events in coastal barrier systems: Storm-wave induced markers. *Quaternary Science Reviews*, *174*, 80–119. https://doi.org/10.1016/j.quascirev.2017.08.026

Haug, G. H., Hughen, K. A., Sigman, D. M., Peterson, L. C., & Röhl, U. (2001). Southward migration of the intertropical convergence zone through the Holocene. *Science*, *293*(5533), 1304–1308. https://doi.org/10.1126/science.1059725

Herrera, R. G., Durán, F. R., Wheeler, D., Martin, E., Prieto, M., & Gimeno, L. (2004). The use of Spanish and British documentary sources in the investigation of Atlantic hurricane incidence in historical times. In R. J. Murnane & K. Liu (Eds.), *Hurricanes and typhoons: Past, present and future* (pp. 149–175).

Holmes, J. A., Street-Peffott, F. A., Ivanovich, M., & Peffott, R. A. (1995). A late Quaternary palaeolimnological record from Jamaica based on trace-element chemistry of ostracod shells. *Chemical Geology*, *124*(1–2), 143–160. https://doi.org/10.1016/0009-2541(95)00032-h

Johnson, D., Beddows, P., Flynn, T., & Osburn, M. (2018). Microbial diversity and biomarker analysis of modern freshwater microbialites from Laguna Bacalar, Mexico. *Geobiology*, *16*(3), 319–337. https://doi.org/10.1111/gbi.12283

Kennett, D. J., Breitenbach, S. F., Aquino, V. V., Asmerom, Y., Awe, J., Baldini, J. U., et al. (2012). Development and disintegration of Maya political systems in response to climate change. *Science*, *338*(6108), 788–791. https://doi.org/10.1126/science.1226299

Knapp, K. R., Kruk, M. C., Levinson, D. H., Diamond, H. J., & Neumann, C. J. (2010). The International Best Track Archive for Climate Stewardship (IBTrACS): Unifying tropical cyclone data. *Bulletin of the American Meteorological Society*, *91*(3), 363–376. https://doi.org/10.1175/2009bams2755.1

Kortum, G., Vecchi, G. A., Hsieh, T.-L., & Yang, W. (2023). Influence of weather and climate on multidecadal trends in Atlantic hurricane genesis and tracks. *Journal of Climate*, *37*(5), 1501–1522. https://doi.org/10.1175/jcli-d-23-0088.1

Kossin, J. P., Camargo, S. J., & Sitkowski, M. (2010). Climate modulation of North Atlantic hurricane tracks. *Journal of Climate*, *23*(11), 3057–3076. https://doi.org/10.1175/2010jcli3497.1

Kossin, J. P., Emanuel, K. A., & Vecchi, G. A. (2014). The poleward migration of the location of tropical cyclone maximum intensity. *Nature*, *509*(7500), 349–352. https://doi.org/10.1038/nature13278

Landsea, C. W., Harper, B. A., Hoarau, K., & Knaff, J. A. (2006). Can we detect trends in extreme tropical cyclones? *Science*, *313*(5786), 452–454. https://doi.org/10.1126/science.1128448

Li, W., Li, L., Ting, M., & Liu, Y. (2012). Intensification of Northern Hemisphere subtropical highs in a warming climate. *Nature Geoscience*, *5*(11), 830–834. https://doi.org/10.1038/ngeo1590

Lin, N., Lane, P., Emanuel, K. A., Sullivan, R. M., & Donnelly, J. P. (2014). Heightened hurricane surge risk in northwest Florida revealed from climatological-hydrodynamic modeling and paleorecord reconstruction. *Journal of Geophysical Research: Atmospheres*, *119*(14), 8606–8623. https://doi.org/10.1002/2014jd021584

Liu, K.-B., & Fearn, M. L. (1993). Lake-sediment record of late Holocene hurricane activities from coastal Alabama. *Geology*, *21*(9), 793–796. https://doi.org/10.1130/0091-7613(1993)021<0793:lsrolh>2.3.co;2

Liu, K.-B., & Fearn, M. L. (2000). Reconstruction of prehistoric landfall frequencies of catastrophic hurricanes in northwestern Florida from Lake sediment records. *Quaternary Research*, *54*(2), 238–245. https://doi.org/10.1006/qres.2000.2166

Malaizé, B., Bertran, P., Carbonel, P., Bonnissent, D., Charlier, K., Galop, D., et al. (2011). Hurricanes and climate in the Caribbean during the past 3700 years BP. *The Holocene*, *21*(6), 911–924. https://doi.org/10.1177/0959683611400198

Martin, E. R., & Schumacher, C. (2011). The Caribbean low-level jet and its relationship with precipitation in IPCC AR4 models. *Journal of Climate*, *24*(22), 5935–5950. https://doi.org/10.1175/jcli-d-11-00134.1

Martinez, C., Goddard, L., Kushnir, Y., & Ting, M. (2019). Seasonal climatology and dynamical mechanisms of rainfall in the Caribbean. *Climate Dynamics*, *53*(1–2), 1–22. https://doi.org/10.1007/s00382-019-04616-4

McCloskey, T. A., & Knowles, J. T. (2009). Migration of the tropical cyclone zone throughout the Holocene. In J. B. Elsner & T. H. Jagger (Eds.), *Hurricanes and climate change* (pp. 169–187).

Medina-Elizalde, M., Burns, S. J., Lea, D. W., Asmerom, Y., von Gunten, L., Polyak, V., et al. (2010). High resolution stalagmite climate record from the Yucatan Peninsula spanning the Maya terminal classic period. *Earth and Planetary Science Letters*, *298*(1–2), 255–262. https://doi.org/10.1016/j.epsl.2010.08.016

Oglesby, R. J., Sever, T. L., Saturno, W., Erickson, D. J., III., & Srikishen, J. (2010). Collapse of the Maya: Could deforestation have contributed? *Journal of Geophysical Research*, *115*(D12). https://doi.org/10.1029/2009jd011942

Otvos, E. G. (2011). Hurricane signatures and landforms—toward improved interpretations and global storm climate chronology. *Sedimentary Geology*, *239*(1–2), 10–22. https://doi.org/10.1016/j.sedgeo.2011.04.014

Pérez, L., Bugja, R., Lorenschat, J., Brenner, M., Curtis, J., Hoelzmann, P., et al. (2011). Aquatic ecosystems of the Yucatan Peninsula (Mexico), Belize, and Guatemala. *Hydrobiologia*, *661*(1), 407–433. https://doi.org/10.1007/s10750-010-0552-9

Pérez-Alarcón, A., Fernández-Álvarez, J. C., Sorí, R., Nieto, R., & Gimeno, L. (2021). The combined effects of SST and the North Atlantic subtropical high-pressure system on the Atlantic basin tropical cyclone interannual variability. *Atmosphere*, *12*(3), 329. https://doi.org/10.3390/atmos12030329

Perry, E., Velazquez-Oliman, G., & Marin, L. (2002). The hydrogeochemistry of the karst aquifer system of the northern Yucatan Peninsula, Mexico. *International Geology Review*, *44*(3), 191–221. https://doi.org/10.2747/0020-6814.44.3.191

Pollock, A. L., Van Beynen, P. E., DeLong, K. L., Polyak, V., Asmerom, Y., & Reeder, P. (2016). A mid-Holocene paleoprecipitation record from Belize. *Palaeogeography, Palaeoclimatology, Palaeoecology*, *463*, 103–111. https://doi.org/10.1016/j.palaeo.2016.09.021

Ridley, H. E., Asmerom, Y., Baldini, J. U., Breitenbach, S. F., Aquino, V. V., Prufer, K. M., et al. (2015). Aerosol forcing of the position of the intertropical convergence zone since AD 1550. *Nature Geoscience*, *8*(3), 195–200. https://doi.org/10.1038/ngeo2353

Scott, D. B., Collins, E. S., Gayes, P. T., & Wright, E. (2003). Records of prehistoric hurricanes on the South Carolina coast based on micropaleontological and sedimentological evidence, with comparison to other Atlantic Coast records. *Geological Society of America Bulletin*, *115*(9), 1027–1039. https://doi.org/10.1130/b25011.1

Street-Perrott, F., Hales, P., Perrott, R., Fontes, J. C., Switsur, V., & Pearson, A. (1993). Late Quaternary palaeolimnology of a tropical marl Lake: Wally wash great Pond, Jamaica. *Journal of Paleolimnology*, *9*(1), 3–22. https://doi.org/10.1007/bf00680032

Studholme, J., Fedorov, A. V., Gulev, S. K., Emanuel, K., & Hodges, K. (2022). Poleward expansion of tropical cyclone latitudes in warming climates. *Nature Geoscience*, *15*(1), 14–28. https://doi.org/10.1038/s41561-021-00859-1

Sullivan, R. M., Van Hengstum, P. J., Coats, S. J., Donnelly, J. P., Tamalavage, A. E., Winkler, T. S., & Albury, N. A. (2021). Hydroclimate dipole drives multi-centennial variability in the western tropical North Atlantic margin during the middle and late Holocene. *Paleoceanography and Paleoclimatology*, *36*(7), e2020PA004184. https://doi.org/10.1029/2020pa004184

Sullivan, R. M., Van Hengstum, P. J., Donnelly, J. P., Tamalavage, A. E., Winkler, T. S., Little, S. N., et al. (2022). Northeast Yucatan hurricane activity during the Maya classic and postclassic periods. *Scientific Reports*, *12*(1), 20107. https://doi.org/10.1038/s41598-022-22756-2

Sullivan, R. M., van Hengstum, P. J., Wallace, E. J., Coats, S., Donnelly, J. P., Korty, R. L., et al. (2024). NOAA/WDS paleoclimatology—Yucatan cenote grain size and tropical cyclone variability data over the last 2500 years [Dataset]. *NOAA National Centers for Environmental Information*. https://doi.org/10.25921/9PCR-BB83

Trouet, V., Harley, G. L., & Domínguez-Delmás, M. (2016). Shipwreck rates reveal Caribbean tropical cyclone response to past radiative forcing. *Proceedings of the National Academy of Sciences*, *113*, 3169–3174. https://doi.org/10.1073/pnas.1519566113

Van Hengstum, P. J., Donnelly, J. P., Fall, P. L., Toomey, M. R., Albury, N. A., & Kakuk, B. (2016). The intertropical convergence zone modulates intense hurricane strikes on the Western North Atlantic margin. *Scientific Reports*, *6*(1), 21728. https://doi.org/10.1038/srep21728

Wallace, E. J., Coats, S., Emanuel, K., & Donnelly, J. P. (2020). Centennial-scale shifts in storm frequency captured in paleohurricane records from The Bahamas arise predominantly from random variability. *Geophysical Research Letters*, *48*(1), e2020GL091145. https://doi.org/10.1029/2020gl091145

Wallace, E. J., Dee, S. G., & Emanuel, K. A. (2021). Resolving long-term variations in North Atlantic tropical cyclone activity using a Pseudo Proxy paleotempestology network approach. *Geophysical Research Letters*, *48*(18), e2021GL094891. https://doi.org/10.1029/2021gl094891

Wallace, E. J., Donnelly, J. P., Van Hengstum, P. J., Winkler, T. S., McKeon, K., MacDonald, D., et al. (2021). 1,050 years of hurricane strikes on Long Island in The Bahamas. *Paleoceanography and Paleoclimatology*, *36*(3), e2020PA004156. https://doi.org/10.1029/2020pa004156

Weaver, M. M., & Garner, A. J. (2023). Varying genesis and landfall locations for North Atlantic tropical cyclones in a warmer climate. *Scientific Reports*, *13*(1), 5482. https://doi.org/10.1038/s41598-023-31545-4

Winkler, T. S., Van Hengstum, P. J., Donnelly, J. P., Wallace, E. J., Sullivan, R. M., MacDonald, D., & Albury, N. A. (2020). Revising evidence of hurricane strikes on Abaco Island (the Bahamas) over the last 700 years. *Scientific Reports*, *10*, 1–17. https://doi.org/10.1038/s41598-020-73132-x

Winkler, T., Van Hengstum, P., Donnelly, J., Wallace, E., Albury, N., D'Entremont, N., et al. (2023). More frequent hurricane passage across the Bahamian Archipelago during the little ice age. *Paleoceanography and Paleoclimatology*, *38*(11), e2023PA004623. https://doi.org/10.1029/2023pa004623

References From the Supporting Information

Blaauw, M., & Christen, J. A. (2011). Flexible paleoclimate age-depth models using an autoregressive gamma process. *Bayesian Analysis*, *6*(3), 457–474. https://doi.org/10.1214/ba/1339616472

Brown, A. L., Reinhardt, E. G., Van Hengstum, P. J., & Pilarczyk, J. E. (2014). A coastal Yucatan sinkhole records intense hurricane events. *Journal of Coastal Research*, *30*, 418–428. https://doi.org/10.2112/jcoastres-d-13-00069.1

Deevey Jr, E. S., & Stuiver, M. (1964). Distribution of natural isotopes of carbon in Linsley Pond and other New England Lakes. *Limnology & Oceanography*, *9*, 1–11. https://doi.org/10.4319/lo.1964.9.1.0001

González, I., & Ochoa, J. (2001). Seismic and meteorological tsunami contributions in the Manzanillo and Cabo San Lucas seiches of September 14, 1995. *Marine Geodesy*, *24*(4), 219–227. https://doi.org/10.1080/014904101753227860

Hodell, D. A., Curtis, J. H., Jones, G. A., Higuera-Gundy, A., Brenner, M., Binford, M. W., & Dorsey, K. T. (1991). Reconstruction of Caribbean climate change over the past 10,500 years. *Nature*, *352*(6338), 790–793. https://doi.org/10.1038/352790a0

Jarvinen, B. R., Neumann, C. J., & Davis, M. A. (1984). A tropical cyclone data tape for the North Atlantic Basin, 1886–1983: Contents, limitations, and uses [NOAA Technical Memorandum NWS NHC 22]. https://repository.library.noaa.gov/view/noaa/7069

Landsea, C. W., & Franklin, J. L. (2013). Atlantic hurricane database uncertainty and presentation of a new database format. *Monthly Weather Review*, *141*(10), 3576–3592. https://doi.org/10.1175/mwr-d-12-00254.1

Lario, J., Spencer, C., Bardají, T., Marchante, A., Garduño-Monroy, V. H., Macías, J., & Ortega, S. (2020). An extreme wave event in eastern Yucatán, Mexico: Evidence of a palaeotsunami event during the Mayan times. *Sedimentology*, *67*, 1481–1504.

Reimer, P. J., Austin, W. E., Bard, E., Bayliss, A., Blackwell, P. G., Ramsey, C. B., et al. (2020). The IntCal20 Northern Hemisphere radiocarbon age calibration curve (0–55 cal kBP). *Radiocarbon*, *62*(4), 725–757. https://doi.org/10.1017/rdc.2020.41

Servicio Sismológico Nacional (SSN). (2020). *Catálogo de sismicidad*. Universidad Nacional Autónoma de México. (UNAM) Retrieved from http://www.ssn.unam.mx/sismicidad/ultimos/

Tamalavage, A. E., Van Hengstum, P. J., Louchouarn, P., Molodtsov, S., Kaiser, K., Donnelly, J. P., et al. (2018). Organic matter sources and lateral sedimentation in a Bahamian karst basin (sinkhole) over the late Holocene: Influence of local vegetation and climate. *Palaeogeography, Palaeoclimatology, Palaeoecology*, *506*, 70–83. https://doi.org/10.1016/j.palaeo.2018.06.014

Truchelut, R. E., Hart, R. E., & Luthman, B. (2013). Global identification of previously undetected pre-satellite-era tropical cyclone candidates in NOAA/CIRES Twentieth-Century reanalysis data. *Journal of Applied Meteorology and Climatology*, *52*(10), 2243–2259. https://doi.org/10.1175/jamc-d-12-0276.1

Van Hengstum, P. J., Maale, G., Donnelly, J. P., Albury, N. A., Onac, B. P., Sullivan, R. M., et al. (2018). Drought in the northern Bahamas from 3300 to 2500 years ago. *Quaternary Science Reviews*, *186*, 169–185. https://doi.org/10.1016/j.quascirev.2018.02.014